Eur. Phys. J. D **46**, 487–492 (2008)
DOI: 10.1140/epjd/e2007-00331-2

THE EUROPEAN PHYSICAL JOURNAL D

# Measurement of angular dependence of M X-ray production cross-sections in Re, Bi and U at 5.96 keV

G. Apaydın[1,a], E. Tıraşoğlu[1], and Ö. Söğüt[2]

[1] Department of Physics, Faculty of Art and Sciences, Karadeniz Technical University, 61080 Trabzon, Turkey
[2] Department of Physics, Faculty of Art and Sciences, Kahramanmaraş Sütçü İmam University, 46100 Kahramanmaraş, Turkey

Received 9 November 2006 / Received in final form 28 March 2007
Published online 12 December 2007 – 

**Abstract.** The M X-ray production differential cross sections in Re, Bi and U elements have been measured at the 5.96 keV incident photon energy in an angular range 135°–155°. The measurements were performed using a $^{55}$Fe source and a Si(Li) detector. The present results contradict the predictions of Cooper and Zare [*Atomic Collision Processes*, Gordon and Breach, New York (1969)] and experimental results of Kumar et al. [J. Phys. B: At. Mol. Opt. **34**, 613 (2001)]. that, after photoionization of inner shells, the vacancy state has equal population of magnetic substates and the subsequent X-ray emission is isotropic, but confirm the predictions of the calculations of Flügge et al. [Phys. Rev. Lett. **29**, 7 (1972)] and experimental results of Sharma and Allawadhi [J. Phys. B: At. Mol. Opt. **32**, 2343 (1999)] and Ertugrul [Nucl. Instrum. Meth. B **119**, 345 (1996)]. Total M X-ray production cross sections from the decay at the 5.96 keV photon energies are found to be in good agreement with the calculated theoretical results using the theoretical values of M shell photoionization cross section.

**PACS.** 32.30.Rj X-ray spectra – 32.80.Aa Inner-shell excitation and ionization

## 1 Introduction

Anisotropy is one of the most problems for characteristic X-rays. Cooper and Zare [1] predicts that all the subshell vacancy states are equally populated after photoionization the magnetic substates, however, Flugge et al. [3], Berezhko et al. [6] and Papp [7] confirm that the population distribution of the magnetic substates of all the subshell vacancy states with $J > 1/2$ are aligned. It is well established that the $L_3$ subshell X-rays emitted following ion-atom collision have anisotropic angular distribution [8–12]. In recent years, limited work has been done on anisotropy of $L_3$ X-ray production cross section for photon-induced. Kahlon et al. [13,14], and Sharma and Allawadhi [4], Ertugrul [5] and Ertugrul et al. [15–17] have obtained strong angular distribution, while the experimental results for anisotropy of $L_3$ X-ray of Kumar et al. [2], and Puri et al. [18] have obtained isotropic distribution.

In a photoionization experiment [19] involving unpolarized incident beam and detection of X-rays in single mode, the state of the ion is axially symmetric with respect to reflection in the plane perpendicular to incident beam. The angular distribution of X-rays emitted takes on from $W(\theta) = (W_x/4\pi)[1 + \beta_2 P_2(\cos\theta)]$, where $W$ is total probability for photon emission in unit time and $P_2(\cos\theta)$ is the second-order Legendre polynomial in $\cos\theta$. The coefficient of anisotropy $\beta_2$ of the photon angular distribution can be expressed as $\beta_2 = \alpha A_{20}$, where $A_{20}$ is the degree of alignment and the coefficient $\alpha$ depend only on $J$ value of the initial and final states of the ionized atom [6]. As shown above, Coster-Kronig transitions between $L_1$ to $L_3$, $L_2$ to $L_3$ subshells have effected on angular distribution of $L_3$ X-rays. For this reason, Kumar et al. [2] and Sharma and Allawadhi [4] have selected ionization energy of $L_3$ subshell at the $E_{inc}$ photon energy ($E_{L_3} < E_{inc} < E_{L_2}$, $E_{L_1}$) to eliminate the Coster-Kronig transition effect. Both Sharma and Allawadhi [4] and Kumar et al. [2] used secondary exciter for the ionization of $L_3$ subshell electrons. However, the experimental results of their studies are opposite to the each other. As well-known, there are the some difficulties of secondary excitation procedure such as, scattering of primary photons, exciting efficiency, fixing with the best uncertainty of the scattering angle.

Kumar et al. [2] have measured differential cross sections of L X-rays for Th and U at 17.8, 25.8 and 46.9 keV photon energies. At the 17.8 keV ($E_{L_3} < 17.8$ keV $< E_{L_2}$, $E_{L_1}$) photon energy, the $L_l$, $L_\alpha$, $L_{\beta 6}$, $L_{\beta 2,15}$ and $L_{\beta 5,7}$ X-ray production differential cross section have been measured at 90°, 130° and 160° angles, at the 25.8 and 46.9 keV photon energies, the $L_l$, $L_\alpha$, $L_\eta$, $L_{\beta 6}$, $L_{\beta 2,4,15}$,

[a] e-mail: gapaydin@ktu.edu.tr

$L_{\beta 1,3,5,7}$, $L_{\beta 9,10}$, $L_{\gamma 1,5}$, $L_{\gamma 2,3,6}$ and $L_{\gamma 4}$ X-ray production differential cross sections have been measured at a 130° angle. Puri et al. [18] have measured differential cross sections of $L_l$, $L_\alpha$, $L_\eta$, $L_{\beta 6}$, $L_{\beta 2,4}$, $L_{\beta 9,10}$, $L_{\gamma 1,5}$ and total $L_\gamma$ X-rays for Th at 22.6 keV using an annular source of Cd-109 and a Si(Li) detector. Sharma and Allawadhi [4] have measured differential cross sections of $L_3$ X-rays ($L_l$, $L_\alpha$, $L_\beta$) for Th and U at emission angles 60°, 70°, 80° and 90° by selective photoionization of the $L_3$ subshell of these elements.

Kahlon et al. [13,14] and Ertugrul et al. [15–17] have measured differential cross sections of $L_l$, $L_\alpha$, $L_\beta$ and $L_\gamma$ X-ray lines in some elements with $79 \leqslant Z \leqslant 92$ at 59.5 keV incident photon energy in an angular range 40°–135°. Papp et al. [12] have investigated angular distribution of different $L_3$ X-ray lines of Ba, Sm and Er experimentally for proton impact at 0.23, 0.28 and 0.35 MeV bombarding energies, respectively, using a Si(Li) detector. He found that the anisotropy parameter ($\beta$) of the $IL_l/IL_\gamma$, $IL_\alpha/IL_\gamma$ and $IL_l/IL_\alpha$ are $-0.137 \pm 0.006$, $-0.026 \pm 0.013$, $-0.083 \pm 0.056$ for Ba, $-0.169 \pm 0.010$, $-0.031 \pm 0.003$, $-0.140 \pm 0.010$ for Sm and $-0.165 \pm 0.013$, $-0.024 \pm 0.005$, $-0.146 \pm 0.011$ for Er, respectively. Papp and Campbell [8] have measured that the anisotropy parameters of $L_l$, $L_{\alpha 1,2}$ and $L_{\beta 2,15}$ for Er are $0.052 \pm 0.016$, $0.016 \pm 0.022$ and $0.012 \pm 0.015$, respectively. The measurements were carried out at 22.5°, 30°, 45°, 60°, 75°, 90°, 105° and 120° and the target of Er was ionized by 8.904 keV unpolarized photons.

Ertugrul et al. [20] have measured $K_\alpha$ and $K_\beta$ X-ray polarization degree and polarization effect on $K_\beta/K_\alpha$ intensity ratio for lanthanides. They have found that $K_\beta$ X-rays are more polarized than $K_\alpha$ X-rays. However, polarization degree for both $K_\alpha$ and $K_\beta$ X-rays are interval 1–3%.

Mehta et al. [21] have measured $L_l$, $L_\alpha$, $L_\eta$, $L_{\beta 6}$, $L_{\beta 1,3}$, $L_{\beta 9,10}$ and $L_\gamma$ X-ray production differential cross section for uranium at 22.6 and 59.5 keV photon energies in angular range 43°–140°. Kahlon et al. [22,23] and Kumar et al. [24] have measured differential cross-sections of $L_3$ for Au and Pb using 59, 57 keV photons and 13.6 keV incident photon energy.

Demir et al. [25] and Sahin et al. [26] have measured M X-ray differential cross section for Pt, Au, Hg, Tl and Pb at 5.96 keV in seven angles ranging from 50° to 110°. The M shell X-ray emission differential cross sections for bismuth have been reported by Kahlon and Mann [27].

Extensive literature search reveals that the individual angular dependence L X-ray production cross sections for many elements and different photon energies have been measured. However, angular dependence M X-ray production cross sections for Re, Bi and U in our scattering angles have not been measured. In this paper, the M X-ray emission in Re, Bi and U following selective ionization 5.96 keV photons energy ($E_M < 5.96$ keV $< E_L$) has been measured. The M X-ray production differential cross sections have been measured at 135°, 140°, 145°, 150°, 155° angles. Total cross sections for the production of these M X-rays have also been deduced and compared with theoretical values.

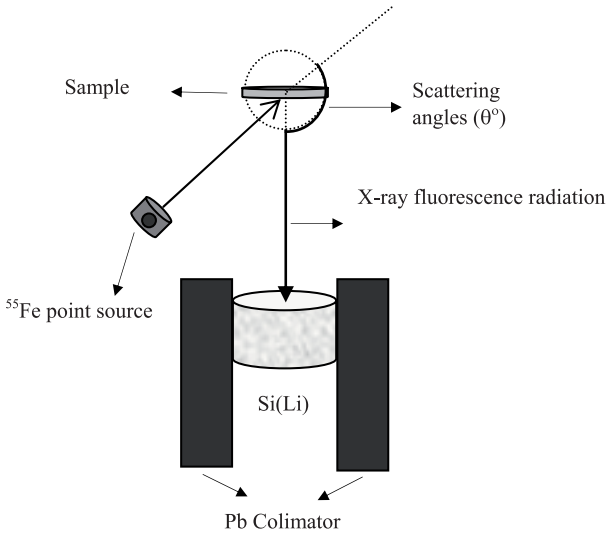


**Fig. 1.** The experimental set-up.

## 2 Experimental

The experimental arrangement is show in Figure 1. The studied compounds were Re, $Bi_2O_3$, $(CH_3COO)_2UO_2 2H_2O$. The purity of commercially obtained materials was better than 99%. Powder samples were sieved using 400 mesh and prepared by supporting on the scotch tape ≅ 10 mg/cm$^2$ thickness. The samples were irradiated by 5.96 keV photons emitted by a 50 mCi $^{55}$Fe radioactive source. The fluorescent X-rays emitted from the target and incident beam are detected and analyzed with a PGT Si(Li) detector (FWHM 160 eV at 5.9 keV, active area 13 mm$^2$, thickness 3 mm and Be window thickness 30 $\mu$m). The output from the preamplifier, with a pulse pile-up rejection capability, was fed to a multi-channel analyzer interfaced with a personal computer provided with suitable software for data acquisition and peak analysis. The live time was taken as 5000 s for all elements. A typical M X-ray spectrum of U taken at 135° is show in Figure 2.

The differential cross section for the emission of M X-rays at angle $\theta$, $d\sigma(M)/d\Omega$ was determined by the method described in detail earlier Kahlon et al. [13,23],

$$\frac{d\sigma_M^\theta}{d\Omega} = N_M^\theta \frac{A}{N}\frac{1}{t}\frac{1}{\beta_M^\theta}\left[\frac{4\pi}{S_\gamma a_\gamma w_1 w_2^\theta \varepsilon_M^\theta}\right] \quad (1)$$

where $N_M^\theta$ is the number of counts/s under the M X-ray peak, $A$ atomic weight, $N$ is Avagadro's number, $t$ is the thickness, $\beta_M^\theta$ is the target self-absorption correction factor, $S_\gamma$ is the number of incident $\gamma$-rays emitted per second from the source, $w_1$ and $w_2^\theta$ are the source-target and target-detector solid angles, $a_\gamma$ is the correction due to absorption of $\gamma$-rays in the air column between the source and target and $\varepsilon_M^\theta$ is the efficiency of the detector for M

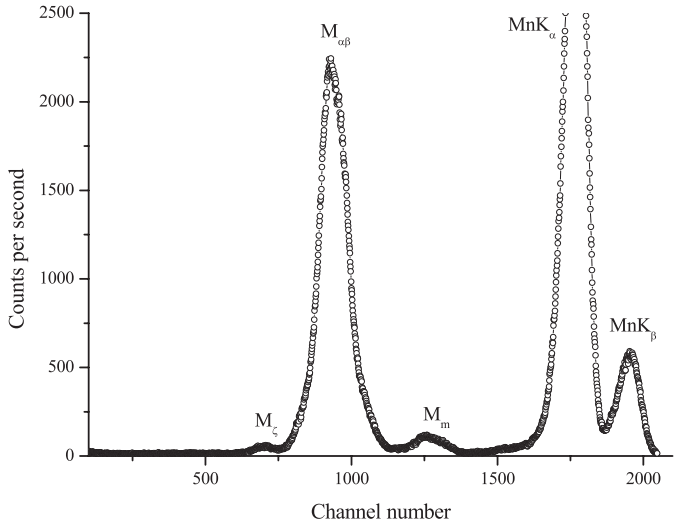


**Fig. 2.** M X-ray spectrum of U excited by 5.96 keV photons.

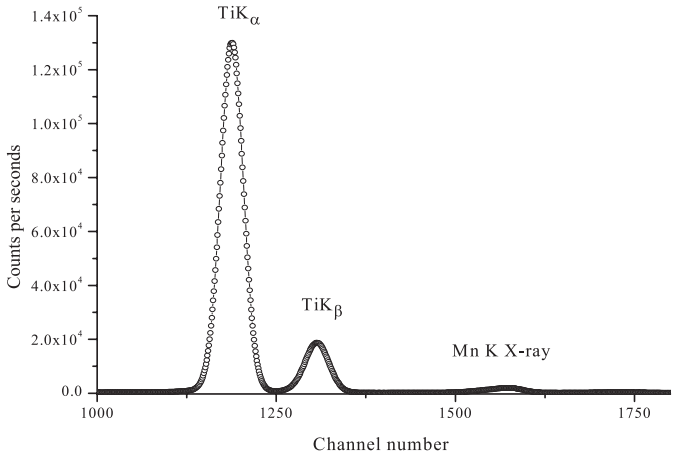


**Fig. 3.** K X-ray spectrum of Ti excited by 5.96 keV photons.

X-rays. The $\beta_M^\theta$ value was calculated from the following equation:

$$\beta = \frac{1 - \exp\left[-\left(\frac{\mu_p}{\cos\theta_1} + \frac{\mu_e}{\cos\theta_2}\right)\right]\rho D}{\left(\frac{\mu_p}{\cos\theta_1} + \frac{\mu_e}{\cos\theta_2}\right)\rho D} \tag{2}$$

where $\mu_p$ and $\mu_e$ are the total mass absorption coefficient of target at primer (5.96 keV) and emitter radiation energy [28], respectively $\theta_1$ and $\theta_2$ are the angles of primer and emitter radiation with sample surface respectively.

The values of factor $4\pi/S_\gamma a_\gamma w_1 w_2^\theta \varepsilon_M^\theta$ were determined experimentally for the same emission angles and different X-ray energies in terms of K X-ray production cross section. For this purpose Re, Bi and U targets were replaced, in turn, with targets of Si, P, S, Cl, K, Ca and Ti and the intensity of K X-rays emitted from each of targets at different angles was recorded. A typical spectrum of Ti X-rays emitted from the target of Ti is shown in Figure 3. This factor is given in the following

$$\frac{4\pi}{S_\gamma a_\gamma w_1 w_2^\theta \varepsilon_M^\theta} = \frac{\sigma_{\mathrm{K}}}{4\pi}\frac{1}{N(\mathrm{K}_i)t\beta_{\mathrm{K}_i}^\theta} \tag{3}$$

where $\sigma_{\mathrm{K}}$ K X-ray production cross sections taken from Scofield [29]. The values of the factor for different emission angles at the weighted mean energies of K X-rays of elements of various targets with atomic number $14 \leqslant Z \leqslant 22$ were determined from equation (3). The values of the factor corresponding to emission angle of $\theta$ are shown in Figure 4.

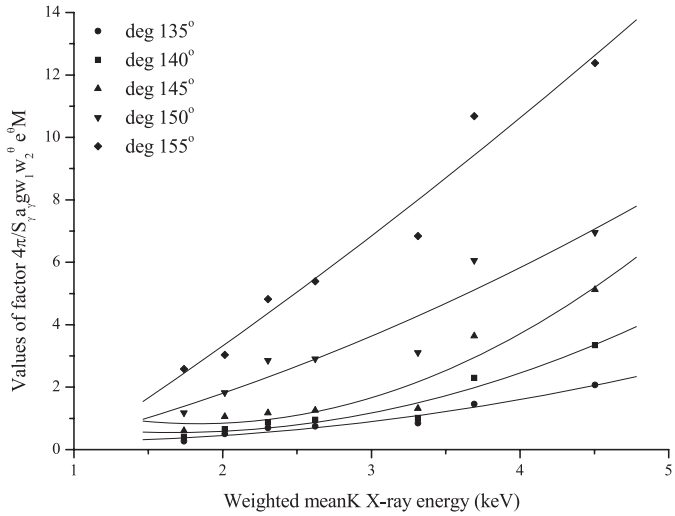


**Fig. 4.** Values of factor $4\pi/S_\gamma a_\gamma w_1 w_2^\theta\ \varepsilon_{\mathrm{M}}^\theta$ at the weighted mean K X-rays energies of elements $14 \leqslant Z \leqslant 22$.

## 3 Total M XRF cross sections

The theoretical values of the total M XRF cross section were calculated using the following relationships:

$$\sigma_{\mathrm{M}_1}^x = \sigma_{\mathrm{M}_1}\omega_1 \tag{4}$$

$$\sigma_{\mathrm{M}_2}^x = (\sigma_{\mathrm{M}_1}\mathrm{S}_{12} + \sigma_{\mathrm{M}_2})\omega_2 \tag{5}$$

$$\sigma_{\mathrm{M}_3}^x = [\sigma_{\mathrm{M}_1}(\mathrm{S}_{13} + \mathrm{S}_{12}\mathrm{S}_{23}) + \sigma_{\mathrm{M}_2}\mathrm{S}_{23} + \sigma_{\mathrm{M}_3}]\omega_3 \tag{6}$$

$$\begin{aligned}\sigma_{\mathrm{M}_4}^x = {} & [\sigma_{\mathrm{M}_1}(\mathrm{S}_{14} + \mathrm{S}_{12}\mathrm{S}_{24} + \mathrm{S}_{13}\mathrm{S}_{34} + \mathrm{S}_{12}\mathrm{S}_{23}\mathrm{S}_{34}) \\ & + \sigma_{\mathrm{M}_2}(\mathrm{S}_{24} + \mathrm{S}_{23}\mathrm{S}_{34}) + \sigma_{\mathrm{M}_3}\mathrm{S}_{34} + \sigma_{\mathrm{M}_4}]\omega_4\end{aligned} \tag{7}$$

$$\begin{aligned}\sigma_{\mathrm{M}_5}^x = {} & [\sigma_{\mathrm{M}_1}(\mathrm{S}_{15} + \mathrm{S}_{12}\mathrm{S}_{25} + \mathrm{S}_{13}\mathrm{S}_3 + \mathrm{S}_{14}\mathrm{S}_{23}\mathrm{f}_{45} \\ & + \mathrm{S}_{12}\mathrm{S}_{23}\mathrm{S}_{35} + \mathrm{S}_{12}\mathrm{S}_{24}\mathrm{f}_{45} + \mathrm{S}_{13}\mathrm{S}_{34}\mathrm{f}_{45} + \mathrm{S}_{12}\mathrm{S}_{23}\mathrm{S}_{34}\mathrm{f}_{45} \\ & + \sigma_{\mathrm{M}_2}(\mathrm{S}_{25} + \mathrm{S}_{24}\mathrm{f}_{45} + \mathrm{S}_{23}\mathrm{S}_{35} + \mathrm{S}_{23}\mathrm{S}_{34}\mathrm{f}_{45}) \\ & + \sigma_{\mathrm{M}_3}(\mathrm{S}_{35} + \mathrm{S}_{34}\mathrm{f}_{45}) + \sigma_{\mathrm{M}_4}\mathrm{f}_{45} + \sigma_{\mathrm{M}_5}]\omega_5\end{aligned} \tag{8}$$

$$\sigma_{\mathrm{M}}^x = \sum_{i=1-5}\sigma_{\mathrm{M}_i}^x \tag{9}$$

where $\sigma_{\mathrm{M}i}$ $(i = 1\text{–}5)$ are the M shell photoionization cross section [28], $\omega_i$ $(i = 1\text{–}5)$ are the M subshell fluorescence

**Table 1.** Measured differential M X-ray cross sections (barns/atom).

| Angles of emission | $\frac{d\sigma^{\theta}_{M}}{d\Omega}$(barns/atom) | | | | | | | | |
|---|---|---|---|---|---|---|---|---|---|
| | Re | | | Bi | | | U | | |
| | I | II | III | I | II | III | I | II | III |
| 135° | $83 \pm 2$ | $75 \pm 2$ | $53 \pm 1$ | $169 \pm 4$ | $158 \pm 4$ | $99 \pm 3$ | $557 \pm 12$ | $537 \pm 12$ | $460 \pm 11$ |
| 140° | $95 \pm 3$ | $87 \pm 2$ | $65 \pm 2$ | $182 \pm 5$ | $171 \pm 4$ | $112 \pm 3$ | $571 \pm 13$ | $551 \pm 12$ | $454 \pm 11$ |
| 145° | $109 \pm 4$ | $101 \pm 4$ | $79 \pm 3$ | $193 \pm 7$ | $182 \pm 6$ | $123 \pm 5$ | $583 \pm 13$ | $563 \pm 12$ | $486 \pm 11$ |
| 150° | $121 \pm 5$ | $113 \pm 4$ | $91 \pm 3$ | $202 \pm 8$ | $191 \pm 7$ | $132 \pm 6$ | $597 \pm 14$ | $577 \pm 13$ | $500 \pm 12$ |
| 155° | $132 \pm 6$ | $124 \pm 5$ | $112 \pm 4$ | $217 \pm 10$ | $205 \pm 10$ | $146 \pm 8$ | $612 \pm 16$ | $592 \pm 14$ | $515 \pm 13$ |

I: Differential cross sections for emission of $M_1$, $M_2$, $M_3$, $M_4$, and $M_5$ subshell X-rays.
II: Differential cross section for emission of $M_3$, $M_4$, and $M_5$ subshell X-rays.
III: Differential cross section for emission of $M_3$, $M_4$, and $M_5$ subshell X-rays when the vacancies transferred from the $M_1$ and $M_2$ subshell are excluded.

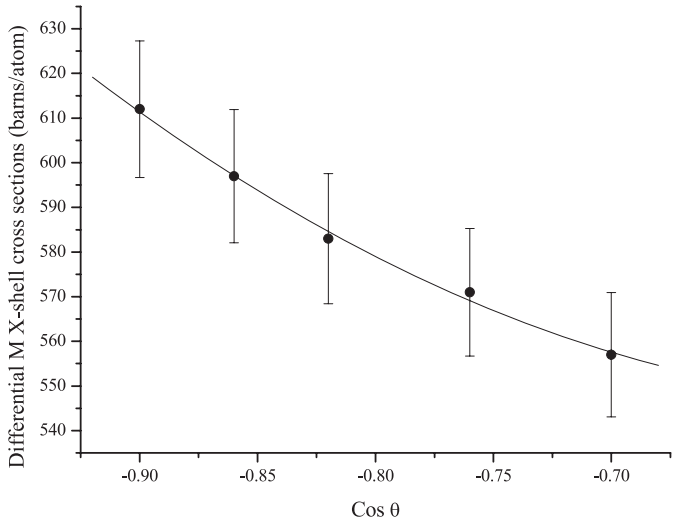


**Fig. 5.** Variation of cross section $d^{\theta}\sigma(\mathrm{M})/d\Omega$ of M shell fluorescent X-rays of U with $\cos\theta$.

yields, $S_{ij}$ ($i$ = 1–3, $j$ = 2–5) are Super Coster-Kronig transition probabilities and $f_{45}$ Coster-Kronig transition probabilities [30–32].

## 4 Results and discussions

The measured X-ray values differential cross section for the emission of $M_i$ ($i = \alpha + \beta$) X-rays at different angles varying from 135° to 155° at intervals of 5° are listed in Table 1. The experimental results are represented graphically as M X-rays production differential cross sections vs. $\cos\theta$ for U plotted in Figure 5. The angular dependence M X-rays production cross sections are found to decrease with increase in the emission angle, showing anisotropic spatial distribution. Present experimental values have been fitted to a second-order polynomial as a function of $\cos\theta$. To the best of our knowledge, no other experimental data are available for comparison with the present results. The percentage error in the measured cross section is attributed to uncertainties in different paremetes in equation (1) namely, error in evaluation of photopeak

**Table 2.** Measured angular distribution coefficients for M$i$ ($i = \alpha + \beta$) lines of Re, Bi and U.

| | Re | Bi | U |
|---|---|---|---|
| $a_0$ | 61.7 | 207.4 | 650.5 |
| $a_1$ | −103.2 | −275.7 | −446.0 |
| $a_2$ | 238.3 | 314.5 | 444.7 |

areas (<3%), $4\pi/\mathrm{S}(\gamma)a(\gamma)w_1w_2^{\theta}\,\varepsilon^{\theta}(\mathrm{M}_i)$ product (<3–5%), targets thickness measurements (<3%) and in the absorption correction factor (<1%). Representing the differential cross-sections for the emission of M-shell X-rays by a Legendre polynominal sum,

$$\frac{d^{\theta}\sigma(\mathrm{M})}{d\Omega} = \sum_{l} a_l P_l(\cos\theta), \tag{10}$$

the observed cross-sections are plotted vs. $\cos\theta$ and fitted to the relation

$$\frac{d^{\theta}\sigma(\mathrm{M})}{d\Omega} = a_0 + a_1\cos\theta + a_2\cos^2\theta, \tag{11}$$

where $a_0$, $a_1$ and $a_2$ are fitting coefficient and listed in Table 2. In light of the fact that the knowledge of M shell Coster-Kronig transition probabilities and fluorescence yields needed in the calculations of reckoned cross sections is inadequate the agreement between experiment and theory is reasonable [33,34]. Assuming the vacancy states produced after photoionization in $M_1$ and $M_2$ subshells with $j = 1/2$ to be unaligned as predicted by Flugge et al. [3] and Baker et al. [35] and later confirmed by Kahlon et al. [13], the values of differential cross sections at various angles for the emission of M X-rays resulting from transitions to $M_3$, $M_4$ and $M_5$ subshells only are found by subtracting $(1/4\pi)[\sigma(\mathrm{M}_1)+\sigma(\mathrm{M}_2)]$ from the measured differential cross section $d^0\sigma(\mathrm{M})/d\Omega$ and are listed in column II of Table 1. $\sigma(\mathrm{M}_1)$ and $\sigma(\mathrm{M}_2)$ are calculated cross sections for production of $M_1$ and $M_2$ subshell X-rays. Nevertheless, some of the vacancies created directly by photoionization of electrons in $M_1$ and $M_2$ subshells are transferred to $M_3$, $M_4$ and $M_5$ subshells through Coster-Kronig transitions before the emission of $M_3$, $M_4$

**Table 3.** Total M shell X-ray fluorescence cross sections, ($\sigma_{\mathrm{M}}^{x}$), (barns/atom).

| Element | | | Other Exp. | Theoretical | | |
|---|---|---|---|---|---|---|
| | Measured | Calculated | Ref. [36] | Refs. [30,31] | Ref. [32] | Refs. [37] |
| Re | $1773 \pm 160$ | 1730 | $1815 \pm 123$ | 1944 | 2003 | 1700 |
| Bi | $3923 \pm 290$ | 4087 | $4503 \pm 242$ | 4334 | 4403 | 4018 |
| U | $10027 \pm 540$ | 9518 | $9790 \pm 592$ | 9304 | – | 9351 |

and $M_5$ subshell X-rays. Assuming the emission of X-rays due to the filling of vacancies transferred from $M_1$ and $M_2$ subshells with $j = 1/2$ to be isotropic, the differential cross sections for the emission of $M_3$, $M_4$ and $M_5$ subshell X-rays due to filling of vacancies created in them directly by photoionization were evaluated by subtracting from the cross-sections listed in column II, the cross section due to the filling of transferred vacancies, and listed in column III of Table 1.

The total cross sections of M-shell X-rays were determined from the angular distribution coefficients ($a_n$) by using the relation [27]

$$\sigma_{\mathrm{M}}^{total} = 2\pi \int_0^{\pi} \sum_{n=0}^{2} a_n \cos^n \theta \sin\theta d\theta. \qquad (12)$$

This relation is rewritten more explicitly as follows:

$$\sigma_{\mathrm{M}}^{total} = 2\pi \left[ \int_0^{\pi} a_0 \sin\theta d\theta + \int_0^{\pi} a_1 \cos\theta \sin\theta d\theta \times \int_0^{\pi} a_2 \cos^2\theta \sin\theta d\theta \right]. \qquad (13)$$

By solving the integrals is obtained

$$\sigma_{\mathrm{M}}^{total} = 4\pi \left( a_0 + \frac{a_2}{3} \right) \qquad (14)$$

where $a_0$ and $a_2$ are as in equation (11) [38]. Using these values of the coefficients, total M shell X-ray cross sections are obtained and are given for present elements in Table 3. It is clear from Table 3 that present values are agreed with theoretical results. Reasonable agreement (to within %2.5–5.3) is calculated and experimental values. According to the present results and earlier experimental [8–20] and theoretical studies [3,6,7], the characteristic X-ray productions cross section from $J \geqslant 1/2$ state is shown angular sensitivity. Furthermore both Papp's prediction and earlier experiment's results show the anisotropy parameter is depend on angular momentum of final state.

Consequently, the angular dependence M X-ray productions cross section is found to increase with in the emission angle showing anisotropic spatial distribution. Because angular dependence M X-ray production cross section worked angles is not found in the literature, the comparison has been not made with other experimental results. Therefore, the results for the elements obtained in the present study constitute the first experimental measurements.

## References


1. J. Cooper, R. Zare, *Atomic Collision Processes* (New York, Gordon and Breach, 1969), vol. XIC, p. 317
2. A. Kumar, S. Puri, J.S. Shahi, M.L. Garg, D. Mehta, N. Singh, J. Phys. B: At. Mol. Opt. **34**, 613 (2001)
3. S. Flugge, W. Mehlhorn, V. Schmidt, Phys. Rev. Lett. **29**, 7 (1972)
4. J.K. Sharma, K.L. Allawadhi, J. Phys. B: At. Mol. Opt. **32**, 2343 (1999)
5. M. Ertugrul, Nucl. Instrum. Meth. B **119**, (1996) 345
6. E.G. Berezhko, N.M. Kabachnik, U.S. Rostovsky, J. Phys. B: At. Mol. Opt. **11**, 1749 (1978)
7. T. Papp, Nucl. Instrum. Meth. B **154**, 300 (1999)
8. T. Papp, J.L. Campbell, J. Phys. B: At. Mol. Opt. **25**, 3765 (1992)
9. A. Gutenkunst, S. Zuccatti, W. Mehlhorn, J. Phys. B: At. Mol. Opt. **27**, 533 (1992)
10. V.P. Petukhov, E.A. Romanovsky, H. Kerkow, Nucl. Instrum. Meth. B **109**, 19 (1996)
11. K. Hino, T. Watanobe, Phys. Rev. A **36**, 5862 (1987)
12. T. Papp, Y. Awaya, A. Hitachi, T. Kambara, Y. Kanai, T. Mizogawa, I. Török, J. Phys. B: At. Mol. Opt. **24**, 3797 (1991)
13. K.S. Kahlon, H.S. Aulakh, N. Singh, R. Mittal, K.L. Allawadhi, B.S. Sood, J. Phys. B: At. Mol. Opt. **23**, 2733 (1990)
14. K.S. Kahlon, H.S. Aulakh, N. Singh, R. Mittal, K.L. Allawadhi, B.S. Sood, Phys. Rev. A **43**, 1455 (1991)
15. M. Ertugrul , R. Durak, E. Tirasoglu, E. Buyukkasap, H. Erdogan, Appl. Spectrosc. Rev. **30**, 219 (1995)
16. M. Ertugrul, E. Buyukkasap, H. Erdogan, Appl. Spectrosc. Rev. **32**, 159 (1997)
17. M. Ertugrul, E. Buyukkasap, Appl. Spectrosc. Rev. **32**, 175 (1997)
18. S. Puri, D. Mehta, J.S. Shahi, M.L. Garg, N. Singh, P.N. Trehan, Nucl. Instrum. Meth. B **152**, 19 (1999)
19. W. Mehlhorn, In X-ray and atomic inner-shell Physics, *American Institute of Physics Conference Proceeding No 94*, edited by B. Crasemann (American Institute of Physics, New York, 1982), p. 53
20. M. Ertugrul, Ö. Şimşek, O. Doğan, E. Öz, Ü. Turgut, Ö. Söğüt, Nucl. Instrum. Meth. B **179**, 465 (2001)
21. D. Mehta, S. Puri, N. Singh, M.L. Garg, P.N. Trehan, Phys. Rev. A **59**, 2723 (1999)
22. K.S. Kahlon, N. Singh, R. Mittal, K.L. Allawadhi, B.S. Sood, Phys. Rev. A **44**, 4379 (1991)
23. K.S. Kahlon, K.L. Allawadhi, B.S. Sood, J. Phys. B: At. Mol. Opt. **24**, 3727 (1991)
24. A. Kumar, M.L. Garg, S. Puri, D. Mehta, N. Singh, X-Ray Spectrom. **30**, 287 (2001)
25. L. Demir, M. Şahin, Ö. Söğüt, Y. Şahin, Rad. Phys. Chem. **59**, 355 (2000)
26. M. Şahin, L. Demir, Y. Kurucu, J. Radioanal. Nucl. Chem. **261**, 415 (2004)

27. K.S. Kahlon, K.S. Mann, J. Electron. Spectrosc. **153**, 92 (2006)
28. E. Strom, I. Israel, Nucl. Data Tables A **7**, 565 (1970)
29. J.H. Scofield, *Theoretical photoionization cross sections from 1 to 1500 keV* (Lawrence Livermore Laboratory, UCRL, 1973), Vol. 51326
30. M.H. Chen, B. Crasemann, H. Mark, Phys. Rev. A **21**, 449 (1980)
31. M.H. Chen, B. Crasemann, H. Mark, Phys. Rev. A **27**, 2989 (1983)
32. E.J. McGuire, Phys. Rev. A **5**, 1043 (1975)
33. K.S. Mann, N. Singh, R. Mittal, K.L. Allawadhi, B.S. Sood, J. Phys. B: At. Mol. Opt. **23**, 2497 (1990)
34. S. Puri, D. Mehta, B. Chand, N. Singh, P.C. Mangal, P.N. Trehan, Nucl. Instrum. Meth. B **73**, 319 (1993)
35. K.R. Baker, F. Tolea, R.W. Fink, J.J. Pinajian, Z. Physik **270**, 1 (1974)
36. G. Apaydin, E. Tirasoglu, U. Cevik, B. Ertugral, H. Baltas, M. Ertugrul, A.I. Kobya, Radiat. Phys. Chem. **72**, 549 (2005)
37. J.H. Hubbell, NISTIR Report **89**, 4144 (1989)
38. Y. Özdemir, Nucl. Instrum. Meth. B **256**, 581 (2007)